Science
AAAS

Supplementary Materials for

A non-canonical inhibitory circuit dampens behavioral sensitivity to light

Takuma Sonoda, Jennifer Y. Li, Nikolas W. Hayes, Jonathan C. Chan, Yudai Okabe, Stephane Belin, Homaira Nawabi, Tiffany M. Schmidt

Correspondence to: tiffany.schmidt@northwestern.edu

This PDF file includes:

Materials and Methods

Animals

All procedures were approved by the Animal Care and Use Committee at Northwestern University. Both male and female mice were used for all experiments except those tracking wheel running activity where only males were used (Fig. 4D-F). For experiments characterizing Gad2-expressing RGCs, Gad2-IRES-Cre (Jackson Laboratory Stock No. 028867) mice were used. Fluorescence *in situ* hybridization experiments utilized *Opn4*$^{Cre/+}$ mice and *Opn4*$^{Cre/+}$*; Gad2*$^{fx/fx}$ mice. For experiments immunolabeling ipRGC axon terminals in the SCN, *Opn4*$^{Cre/+}$, *Opn4*$^{Cre/+}$, and Ai34 (Jackson Laboratory Stock No. 012570) mice were used. Acute brain slice recordings were made using Ai32 (Jackson Laboratory Stock No. 012569) mice. Behavioral experiments in Fig. 4 were conducted using littermates from an *Opn4*$^{Cre/+}$*; Gad2*$^{fx/fx}$ x *Gad2*$^{fx/fx}$ mating. Behavioral experiments in Fig. S15 were conducted using *Gad2*$^{fx/fx}$ mice and WT mice.

Viral infection

Mice between P30-40 were anesthetized by intraperitoneal (IP) injection of Avertin (2,2,2-Tribromoethanol) and a 30-gauge needle was used to open a hole in the ora serrata. Each eye was injected with 1µL of AAV using a custom Hamilton syringe (Borghuis Instruments) with a 33-gauge needle (Hamilton). Animals showing lack of/incomplete retinal infection in Gad2-IRES-Cre; AAV2/hSyn-FLEX-Chrimson-tdT (n = 5) were excluded from further analysis of projection patterns. The AAV2/SNCG-Cre-HA and AAV2/SCNG-hPLAP were newly generated for this study. Expression of Cre and human phosphatase alkaline expression by AAV2 vectors are driven by the human regulatory region of gamma synuclein (SNCG) promotor (*23*). This promotor shows robust and RGC-specific expression of the transgene.

Below is a table detailing viruses used in this study.

Purpose	Virus (AAV2)	Bilateral/ Unilateral	Source
To characterize projections of Gad2-expressing RGCs (Fig. 1)	hSyn-FLEX-Chrimson-tdT	Unilateral	UNC vector core
Label cell bodies of Gad2-expressing RGCs (Fig. 1)	hSyn-DIO-mCherry	Bilateral	Addgene viral prep #50459-AAV2
Labeling ipRGCs for axon terminal immunolabeling (Fig. 2)	hSyn-FLEX-Chrimson-tdT	Bilateral	UNC vector core
Expressing Cre in the retina (Fig. 2 and Fig. 3)	pgk-Cre	Bilateral	UNC vector core
Expressing Cre specifically in RGCs (Fig. S12)	SNCG-Cre-HA	Unilateral	Dr. Homaira Nawabi/Dr. Stephane Belin
Control virus for SNCG-Cre virus (Fig. S12)	SNCG-hPLAP	Unilateral	Dr. Homaira Nawabi/Dr. Stephane Belin

Brain histology and analysis of axon terminal immunolabeling

Mice were anesthetized by IP injection of Avertin and transcardially perfused with PBS followed by 4% paraformaldehyde (Electron Microscopy Sciences) in PBS. Brains were then dissected and postfixed in 4% paraformaldehyde overnight at 4°C. Brains were washed in PBS and blocked by making a coronal cut at the level of the inferior colliculus. For experiments determining projection patterns of RGCs, 100μm coronal sections were then made from rostral to caudal using a Leica VT1000 S vibratome. Sections were mounted directly onto glass slides and allowed to dry. Slides were then coverslipped using Vectashield mounting medium (Vector Laboratories) and imaged using a Leica SPE5500 scanning confocal microscope. Animals with poor viral infection were excluded.

For axon terminal immunolabeling experiments, 50μm coronal sections through the SCN were made using a Leica VT1000 S vibratome. Floating sections were collected in PBS and blocked in 6% normal goat serum in 0.3% Triton PBS overnight at 4°C. Sections were then

transferred to primary antibody solution containing rabbit anti-dsRed (1:1000, Takara, Catalog #: 632496, RRID:AB_10013483), mouse anti-Gad65 (1:1000, Abcam, Catalog #: ab26113, RRID:AB_448989), and guinea-pig anti-synapsin 1/2 (1:500, Synaptic Systems, Catalog #: 106 004, RRID:AB_1106784) in 0.3% Triton PBS with 3% normal goat serum for 2 nights at 4°C. Sections were washed in PBS for 3x30 minutes at room temperature (RT) and transferred to secondary antibody solution overnight at 4°C. Secondary antibody solution contained Alexa 488 goat anti-mouse (1:1000, Thermo, Catalog #: A-11001, RRID:AB_2534069), Alexa 546 goat anti-rabbit (1:1000, Thermo, Catalog #: A-11035, RRID:AB_143051), and Alexa 647 goat anti-guinea pig (1:1000, Thermo, Catalog #: A-21450, RRID: AB_141882) in 3% normal goat serum in 0.3% Triton PBS. Sections were then washed in PBS at RT and mounted on glass cover slides with ProLong Glass Antifade Mountant (Thermo). SCN sections were imaged on a Leica SP8 confocal microscope in the Biological Imaging Facility at Northwestern University. High magnification images (57.22 x 57.22µm images with a pixel size of 58.22nm) were taken using a 63x oil immersion objective.

For analysis, all channels were first filtered by fitting the fluorescence intensity distribution of each image with a half-normal distribution and using a threshold that was 3 standard deviations away from 0. The tdTomato channel, which labeled ipRGC axons, was first segmented to discern objects resembling axon terminals. The image was binarized and subsequently eroded and dilated using a disk structuring element that was 0.5µm in diameter. A Euclidean distance transform was then performed followed by watershed segmentation. Objects were only considered synaptic terminals if they exhibited more than 50% colocalization with the synapsin channel. ipRGC synaptic terminals (objects that are both tdTomato+ and synapsin+) were considered Gad2-immunoreactive if they colocalized with the Gad2 channel by more than 80%.

Retinal histology

To isolate retinas, mice were anesthetized by IP injection of Avertin and sacrificed by cervical dislocation. Eyes were then enucleated and retinas were dissected in PBS. A large relieving cut was made in the nasal margin of the eyecup prior to removing the retina for experiments in which retinal orientation was tracked. Retinas were fixed in 4% paraformaldehyde in PBS for 30-60 minutes at RT and washed in PBS for 1.5 hours (3x30 minutes). Retinas were then blocked at 4°C overnight in 6% normal goat serum in 0.3% Triton PBS prior to incubating in primary antibody solution for 2-3 nights at 4°C. Then, retinas were washed in PBS for 1.5 hours (3x30 minutes) at RT and incubated in secondary antibody solution for 2-3 hours at RT. Retinas were washed and mounted using Fluoromount (Sigma).

Primary and secondary antibody solutions were made in 3% normal goat serum in 0.3% Triton PBS. For experiments staining AAV infected retinas for melanopsin, rabbit anti-melanopsin (1:2000, Advanced Targeting Systems, Catalog #: AB-N38, RRID:AB_1608077) and chicken anti-mCherry (1:1000, Abcam, Catalog #: ab125096, RRID:AB_11133266) were included in the primary antibody solution, which was followed by a secondary staining with Alexa 488 goat anti-rabbit (1:500, Thermo, Catalog #: A-11008, RRID:AB_143165) and Alexa 568 goat anti-chicken (1:500, Thermo, Catalog #: A-11041, RRID:AB_2534098). For experiments staining AAV infected retinas for RBPMS and Brn3a, rabbit anti-RBPMS (1:1000, Millipore, Catalog #: ABN1376, RRID:AB_2687403), chicken anti-mCherry (1:1000, Abcam, Catalog #: ab205402, RRID:AB_2722769), and mouse anti-Brn3a (1:500, Millipore, Catalog #: MAB1585, RRID:AB_94166) were included in the primary antibody solution. Alexa 488 goat anti-rabbit (1:500, Thermo, Catalog #: A-11008, RRID:AB_143165), Alexa 568 goat anti-chicken (1:500, Thermo, Catalog #: A-11041, RRID:AB_2534098), and Alexa 647 goat anti-mouse (1:500, Thermo, Catalog #: A-21235, RRID:AB_2535804) were included in the secondary antibody solution.

RNA fluorescence *in situ* hybridization (FISH) in retinal sections

Retinal sections were prepared by dissecting eyecups from mice in nuclease-free PBS and fixing eyecups in 4% paraformaldehyde solution in PBS for 24 hours at 4°C. Eyecups were then washed in PBS and cryoprotected in a 30% sucrose solution in PBS overnight at 4°C. Eyecups were then embedded and frozen in OCT using dry ice. 20µm sections were made on a Leica CM1950 cryostat and mounted directly onto SuperFrost Plus slides (Fisher). The tissue was processed according to the RNAscope Multiplex Fluorescent v2 assay (Advanced Cell Diagnostics) instructions provided by the manufacturer. Probes for Mm-Gad2 (Catalog Number: 439371) and Mm-Opn4-C2 (Catalog number: 438061-C2) were used. Gad2 probes were labeled with Cyanine 5 (Catalog number: NEL745001KT) and Opn4 probes were labeled with Cyanine 3 (Catalog number: NEL744001KT) using the TSA Plus Fluorescence kits (Akoya Biosciences). The tissue was then incubated in DAPI solution (Sigma) prepared in nuclease-free PBS for 10 minutes and cover slipped using ProLong Glass Antifade Mountant (Thermo).

Retinal sections were imaged on a Leica SP8 confocal microscope in the Biological Imaging Facility at Northwestern University. For quantification, high magnification images (36.97µm x 36.97µm with a pixel size of 72.2nm) with a z-stack size of 0.66µm (in 0.33µm increments) were taken. Because ipRGCs are a sparse population of RGC, it was possible to capture images that only included a single ipRGC per image. This made automated quantification of Gad2 puncta within ipRGCs possible without using a clustering algorithm to establish ROIs around multiple ipRGCs in the same image. Because the optical sectioning was not perfect, out of focus puncta were excluded from neighboring cells by capturing small z-stack sizes around the midportion of ipRGCs.

Quantification of RNA FISH experiments

To establish a boundary around each ipRGC automatically, a custom script was written in MATLAB (MathWorks) to draw regions of interest (ROIs) around Opn4 mRNA signal (depicted in figure form in Fig. S5). To do this, a Determinant of Hessian algorithm was first used to

roughly detect blobs in the images of Opn4 signal using the 'vl_covdet' function in the VLFeat computer vision toolbox for MATLAB (vlfeat.org). An ellipse was drawn based on a principle component analysis (PCA) of the positions of the detected blobs representing Opn4 signal. Outlier detections that resided outside this ellipse were then discarded and a more refined ellipse was drawn by performing PCA again with only the inlier detections. To achieve an even greater precision ROI than an ellipse, the Maximally Stable Extrema Regions (MSER) algorithm was then performed on the image of Opn4 signal to more comprehensively detect all potential Opn4 signal (using the 'vl_mser' function in the VLFeat computer vision toolbox for MATLAB). Because the MSER algorithm may detect noise, only the MSER regions detected within the inlier ellipse produced by the earlier PCA on inlier detections were used. A convex hull was then constructed around these inlier MSER regions, resulting in a polygon used to define the Opn4 ROI. To quantify the number of Gad2 puncta that reside within each Opn4 ROI, Gad2 puncta were first quantified by convolving the image with a gaussian function. We then counted the number of puncta that resided within the ROI using the 'inpolygon' function in MATLAB. Codes used for RNAscope analysis are accessible at github.com/schmidtlab-northwestern.

Analyses were performed on 236 cells from 2 retinas of *Opn4*$^{Cre/+}$; *Gad2*$^{fx/fx}$ mice and 424 cells from 4 retinas of *Opn4*$^{Cre/+}$ mice. To quantify the proportion of Gad2-expressing ipRGCs, a threshold was established by measuring the 100th percentile value of Gad2 puncta in ipRGCs in *Opn4*$^{Cre/+}$; *Gad2*$^{fx/fx}$ retinas (Fig. S7). ipRGCs that had more Gad2 puncta than this threshold in *Opn4*$^{Cre/+}$ mice were deemed Gad2-expressing (Gad2+).

Solutions for electrophysiology

To prepare acute brain slices, two different solutions were used as previously described (*29*). The first was an "NMDG recovery solution" which contained (in mM): 93 N-Methyl-D-glucamine (NMDG), 2.5 KCl, 1.2 NaH_2PO_4, 30 $NaHCO_3$, 20 HEPES, 25 glucose, 5 sodium ascorbate, 2 thiourea, 3 sodium pyruvate, 10 $MgSO_4$, 0.5 $CaCl_2$. pH was adjusted to 7.4 using 10M HCl. The

second was a HEPES buffered artificial cerebral spinal fluid (aCSF) which contained (in mM): 92 NaCl, 2.5 KCl, 1.2 NaH_2PO_4, 30 $NaHCO_3$, 20 HEPES, 25 glucose, 5 sodium ascorbate, 2 thiourea, 3 sodium pyruvate, 2 $MgSO_4$, 2 $CaCl_2$. pH was adjusted to 7.4 using 1M NaOH.

Recordings were made in aCSF, which contained (in mM): 125 NaCl, 2.5 KCl, 1.25 NaH_2PO_4, 25 $NaHCO_3$, 25 glucose, 2 $CaCl_2$, 1 $MgCl_2$. Tetrodotoxin (TTX, 500nM, Tocris) and 4-aminopyridine (4-AP, 500µM, Sigma) were used to measure monosynaptic currents elicited by photo-activating ipRGC axons. NBQX (20µM, Tocris) and D-APV (50µM, Tocris) were bath applied to block glutamate receptors. SR 95531 (Gabazine, 25 µM, Tocris) was bath applied to block $GABA_A$ receptors. A cesium-based internal solution was used which contained (in mM): 125 Cs-methanesulfonate, 10 CsCl, 1 $MgCl_2$, 5 EGTA, 10 Na-HEPES, 2 Na_2-ATP, 0.5 Na-GTP, 10 Phosphocreatine, 2 QX-314, and 0.3% Neurobiotin (Vector Laboratories).

Acute brain slice recordings and analyses

Mice between 1-3 months of age were anesthetized by IP injection of Avertin and decapitated into ice cold aCSF. 275-300µm coronal sections were cut in ice cold aCSF using a Leica VT1000 S vibratome. Sections were then incubated in NMDG recovery solution at 32°C for 10-15 minutes and then allowed to recover in HEPES buffered aCSF for at least 30 minutes at RT prior to recording. Only 1-2 SCN sections could be prepared from each animal. Recordings were made in aCSF at 26-28°C.

Recordings were made using borosilicate pipettes (Sutter Instruments) with resistances between 5-7MΩ. Data were collected using a Multiclamp 700B amplifier (Molecular Devices) with pClamp 10 acquisition software. Reported voltages are corrected for a 10mV liquid junction potential between the aCSF and cesium internal solution. To photoactivate ipRGC axons expressing ChR2, a 1ms 470nm light stimulus (~2mW/mm^2) was delivered via an LED light source.

To ensure that recorded neurons were in the SCN, sections were fixed overnight in a 2-4% paraformaldehyde solution in PBS at 4°C. Sections were then washed in PBS for at least 2 hours in PBS and then blocked overnight in 6% goat serum in 1% Triton PBS at 4°C. Sections were then incubated in primary antibody solution for 2 nights at 4°C. Primary antibody solution contained chicken anti-GFP (1:1000, Abcam, Catalog #: ab13970, RRID:AB_300798) and Streptavidin conjugated to Alexa 546 (1:1000, Thermo, Catalog #: S-11225, RRID:AB_2532130) and rabbit anti-VIP (1:500, Immunostar, Catalog #: 20077, RRID:AB_572270) in blocking solution. Then, sections were washed for 1.5 hours (3x30 minutes) at RT and incubated in secondary antibody solution overnight at 4C. Secondary antibody solution contained Alexa 488 goat anti-chicken(1:500, Thermo, Catalog #: A-11039, RRID:AB_142924) and Streptavidin conjugated to Alexa 546 (1:1000, Thermo, Catalog #: S-11225, RRID:AB_2532130) and Alexa 647 goat anti-rabbit (1:500, Thermo, Catalog #: A-21245, RRID:AB_2535813). Sections were washed in PBS and mounted on glass slides using ProLong Glass Antifade Mountant (Thermo). Location was documented for 72/79 recorded SCN neurons (Fig. S8).

EPSC and IPSC amplitudes were measured by averaging 500µs around the peak of the elicited current and subtracting the baseline current. Synaptic latency was measured as the time at which the derivative of the current trace (dI/dt) reached a value of 15 pA/ms. This method of calculating latency was used instead of measuring the timepoint the current deviated 3-4 standard deviations above baseline because the standard deviation of the baseline current was much larger when cells were voltage clamped at 0mV due to the large amount of spontaneous IPSCs in the SCN.

Pupillometry

For PLR experiments, experiments were performed between Zeitberger times 2 and 10. Experimenters were blind to the genotype of all animals. Consensual PLR was measured by delivering a 470nm light stimulus to one eye while simultaneously recording the other eye using

a Sony Handycam camcorder. An LED light source was band passed using a 470nm bandpass filter (Thorlabs) and light intensity was attenuated using neutral density filters (Thorlabs). Mice were dark-adapted for at least 30 minutes prior to any light exposure and were then manually restrained by hand. A 5-10 second baseline recording was taken prior to delivering the 20 second light stimulus. The order in which animals were tested after dark adaptation was randomized. Pupil area was quantified post hoc using the oval tool in ImageJ. Steady-state pupil area was then calculated by averaging the pupil area during the last 10 seconds of the stimulus. In analyses looking at the time course of PLR, data were fit using a single exponential decay function to measure the time constant tau in Graphpad Prism 6.

Optokinetic tracking

Spatial frequency thresholds were assessed using the virtual OptoMotry system (Cerebral Mechanics, Lethbridge, Alberta) as described previously (*30, 31*). A vertical sine wave grating was projected as a virtual cylinder in 3D coordinate space on computer monitors arranged in a quadrangle around a testing arena. Unrestrained animals were placed individually on an elevated platform at the epicenter of the arena. Experimenters were blind to the genotype of all animals. The experimenter used a video image of the arena from above to view the animal, and followed the position of its head in real time to determine when the mouse “tracked” which was defined as when the head and neck movements of the animals moved in the same direction as the drifting grating. Animals were presented with stimuli of increasing spatial frequencies to assess the spatial frequency threshold of the animal in both clockwise and counterclockwise directions. Because the temporal-to-nasal stimulus movement in the visual field evokes tracking, clockwise and counterclockwise stimulation can be used to assess the spatial frequency threshold of each eye individually (*30*). All measurements were conducted using a cylinder rotation of 12°/sec, and these thresholds were measured for each eye and averaged for each mouse.

Voluntary wheel running behavior

Wheel running activity was recorded by individually housing male mice in cages with a running wheel. Activity was recorded using ClockLab Data Collection software (Actimetrics). Mice were first exposed to a 12:12 light dark (LD) cycle with 100 lux light during the light phase for 3 weeks. Then, the LED light source was attenuated to 1.5lux using neutral density sheets (Rosco) while simultaneously exposing animals to a 6-hour phase advance. After 4 weeks, the light was attenuated to 0.2 lux while exposing animals to another 6-hour phase advance. Mice were kept at the 0.2lux LD cycle for 4 weeks. Mice were genotyped after recording wheel running activity to avoid any experimenter bias during data collection. Mice that stopped running during the experiment were excluded. All data analysis was performed using ClockLab 6 analysis software (Actimetrics). Circadian amplitude, total activity, percent activity in light and onset error were measured in the 10 days preceding each phase advance.

Statistical comparisons

For behavior experiments, a non-parametric, Mann-Whitney U test was used because sample sizes were not large enough to assume a normal distribution.

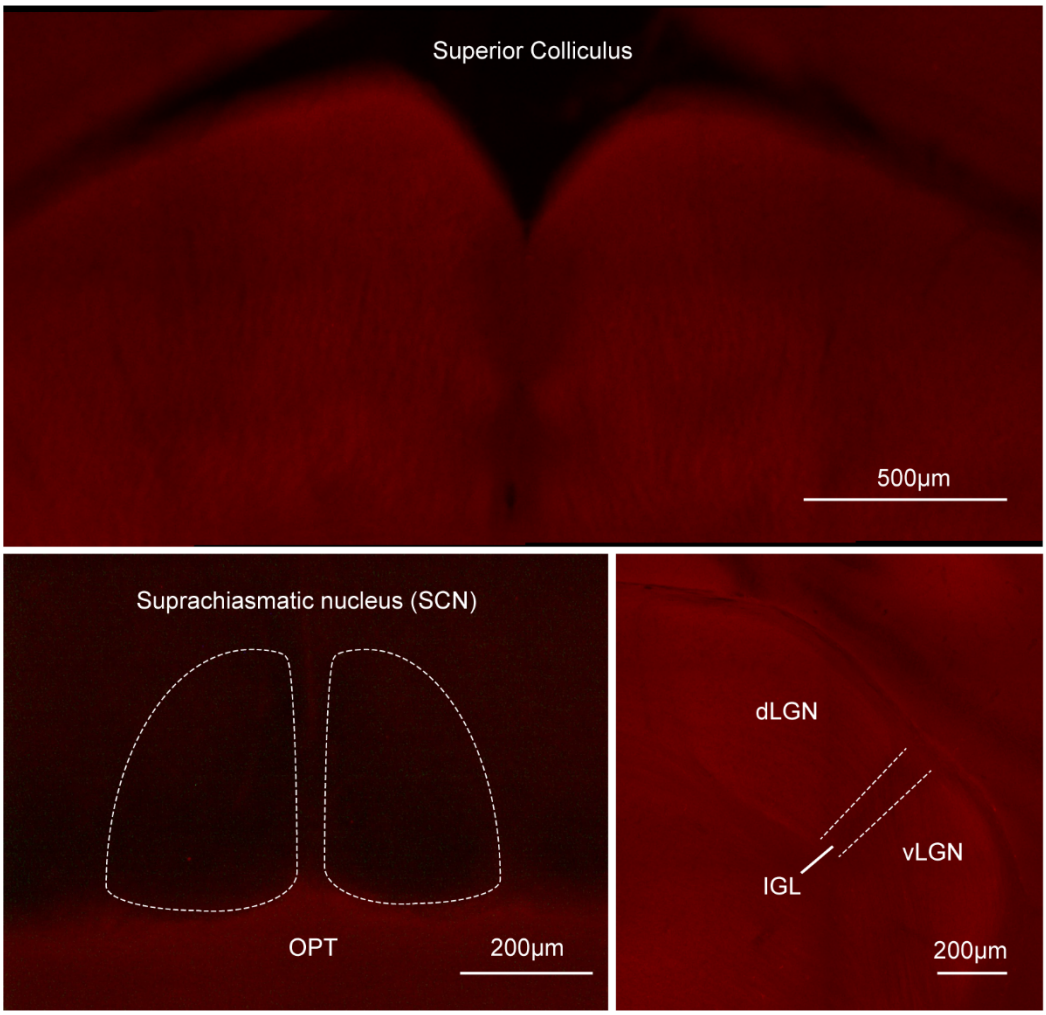

Fig. S1. No labeling observed in WT animals eye injected with AAV2/hSyn-FLEX-Chrimson-tdTomato virus.

Example images of the superior colliculus, suprachiasmatic nucleus (SCN) and the lateral geniculate nucleus (LGN) in a WT mouse eye injected with AAV2/hSyn-FLEX-Chrimson-tdT virus. No axon labeling was observed in 3/3 animals.

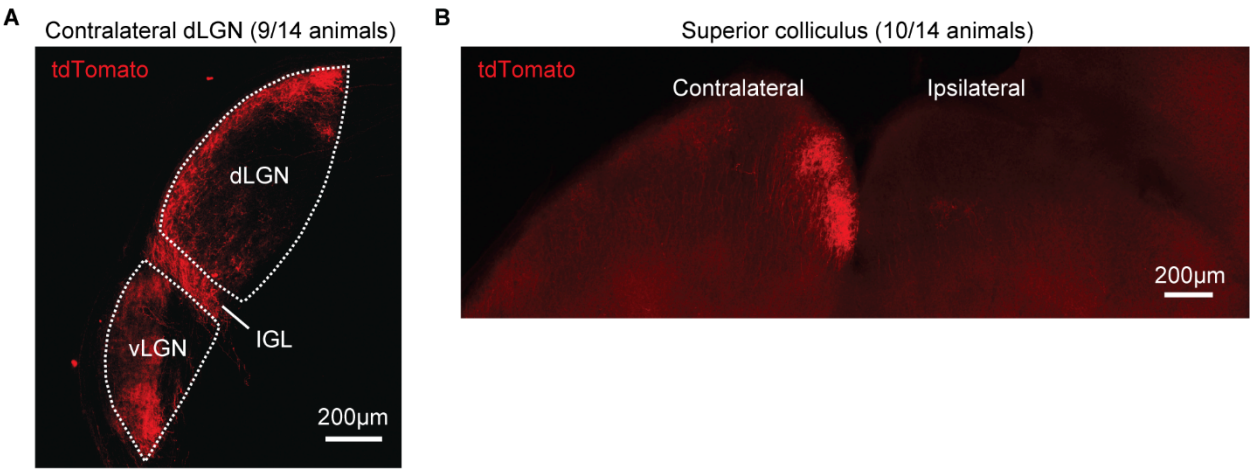

Fig. S2. Image forming targets RGCs labeled in Gad2-IRES-Cre mice.

(**A and B**) Projections to the contralateral shell of the dorsal lateral geniculate nucleus (dLGN, **A**) and the posterior medial superior colliculus (**B**) were observed in a proportion of Gad2-IRES-Cre mice intravitreally injected with AAV2/hSyn-FLEX-Chrimson-tdTomato.

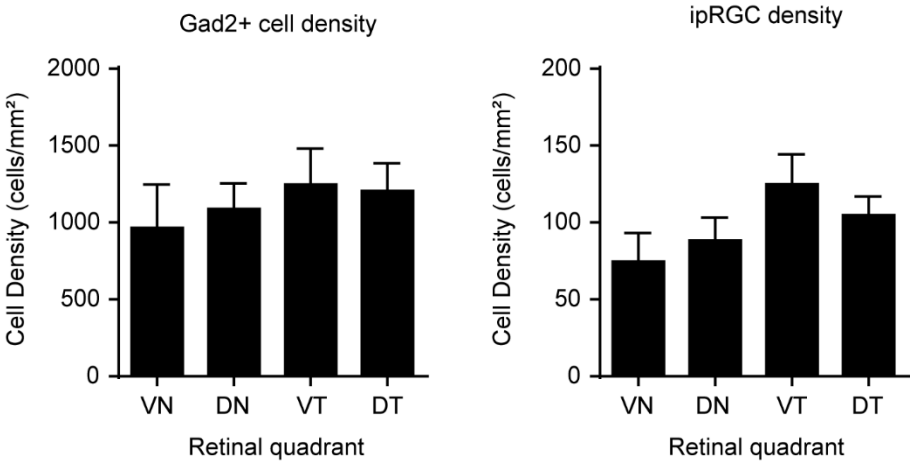

Fig. S3. Density of Gad2+ and of ipRGCs in different retinal quadrants.

The density of Gad2+ cells (left) and melanopsin-immunoreactive cells (ipRGCs, right) labeled in different retinal quadrants. Data are quantified from same images used to quantify the percentage of Gad2+ ipRGCs in Fig. 1E-G. N = 6 retinas. VN (ventral-nasal), DN (dorsal-nasal), VT (ventral-temporal), DT (dorsal-temporal). Data are mean ± SD.

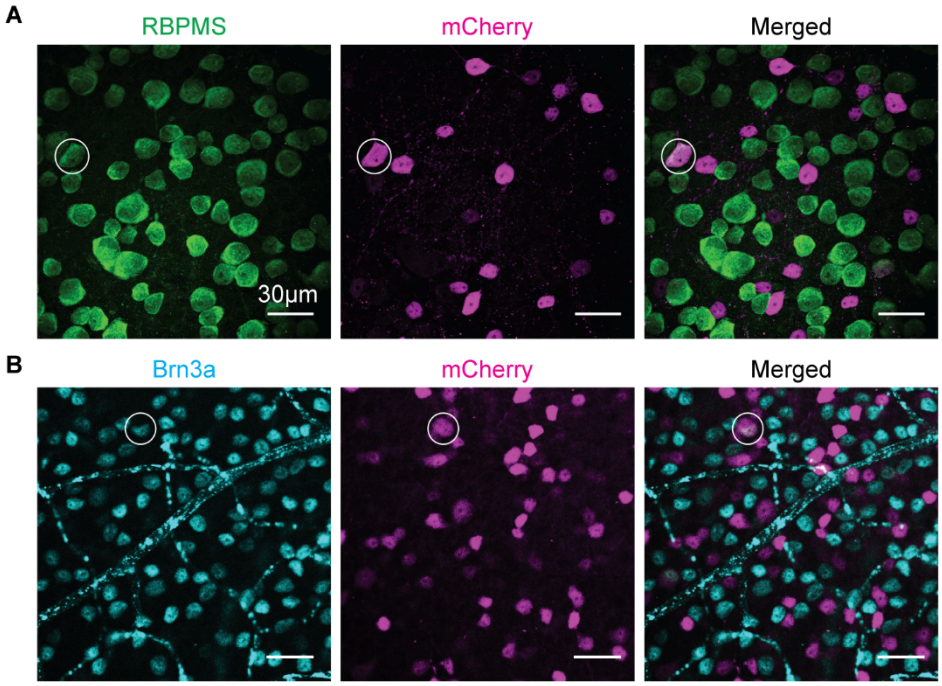

Fig. S4. 1% of all RGCs and 0.6% of Brn3a+ RGCs are Gad2+.

(A) Example images showing an infected retina from a Gad2-IRES-Cre mouse eye injected with AAV2/hSyn-DIO-mCherry immunolabeled for RBPMS (green), which labels all RGCs. Solid white circle indicates a Gad2+ RGC. 0.98 ± 0.31% of RBPMS+ cells were Gad2+ (mean ± SD, total of 19,727 cells counted in 5 retinas).

(**B**) Example images showing an infected retina from a Gad2-IRES-Cre mouse eye injected with AAV2/hSyn-DIO-mCherry immunolabeled for Brn3a (cyan), which is a pan-RGC marker that does not label ipRGCs. The white solid circle indicates a Brn3a+ RGC that is Gad2+ 0.63 ± 0.11% of Brn3a+ cells were Gad2+ (mean ± SD, total of 9236 cells counted in 3 retinas).

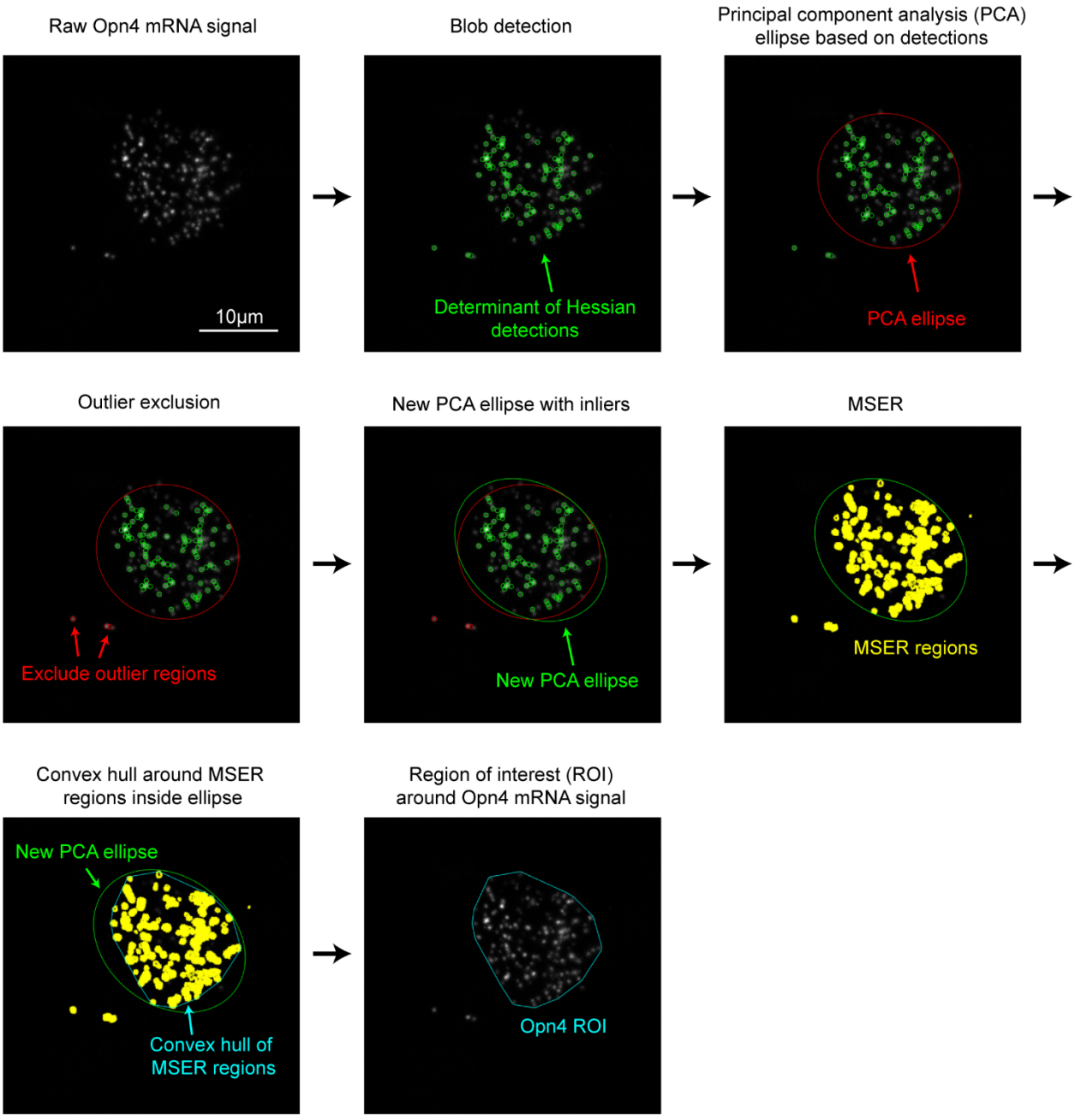

Fig. S5. Establishing regions of interest (ROIs) around Opn4 mRNA signal.

An example of the general workflow used to establish ROIs around Opn4 mRNA signal from RNA fluorescence *in situ* hybridization experiments (see methods for a detailed description).

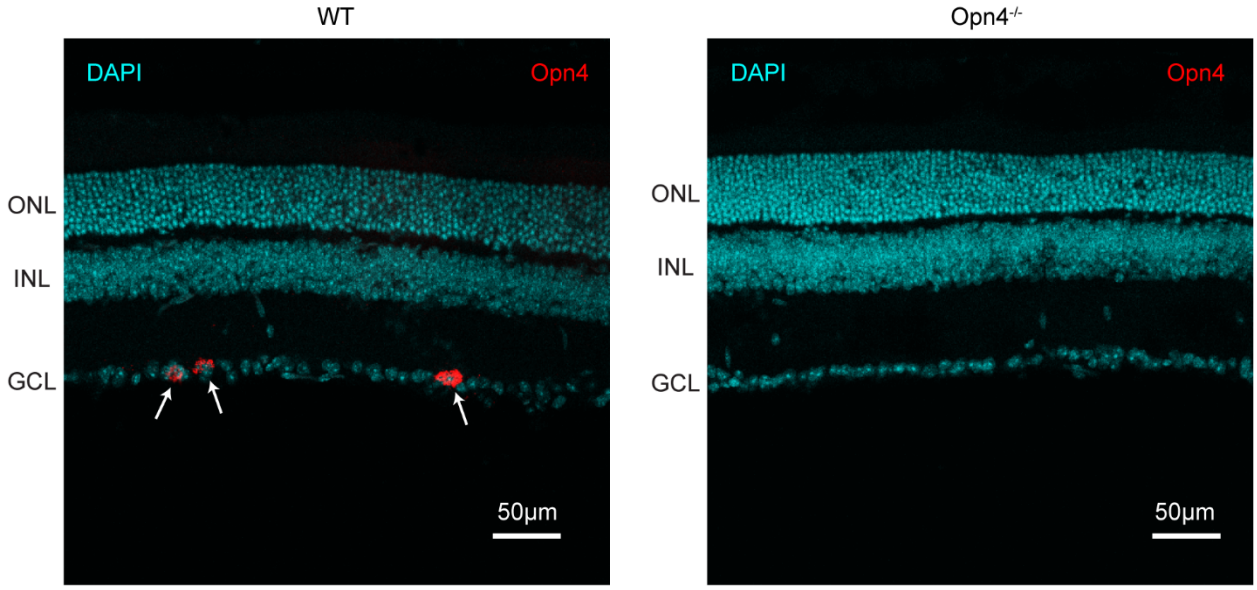

Fig. S6. Opn4 knockout control for RNA fluorescence *in situ* hybridization experiments.

Example images of retinal sections from WT and Opn4 knockout (*Opn4*$^{-/-}$) animals. A probe to detect Opn4 mRNA (red) was used. Consistent labeling was observed in retinal sections from 2 WT retinas and no labeling was observed in retinal sections from 4 Opn4$^{-/-}$ retinas. Arrows indicate Opn4+ signal (putative ipRGCs). ONL (outer nuclear layer), INL (inner nuclear layer), GCL (ganglion cell layer).

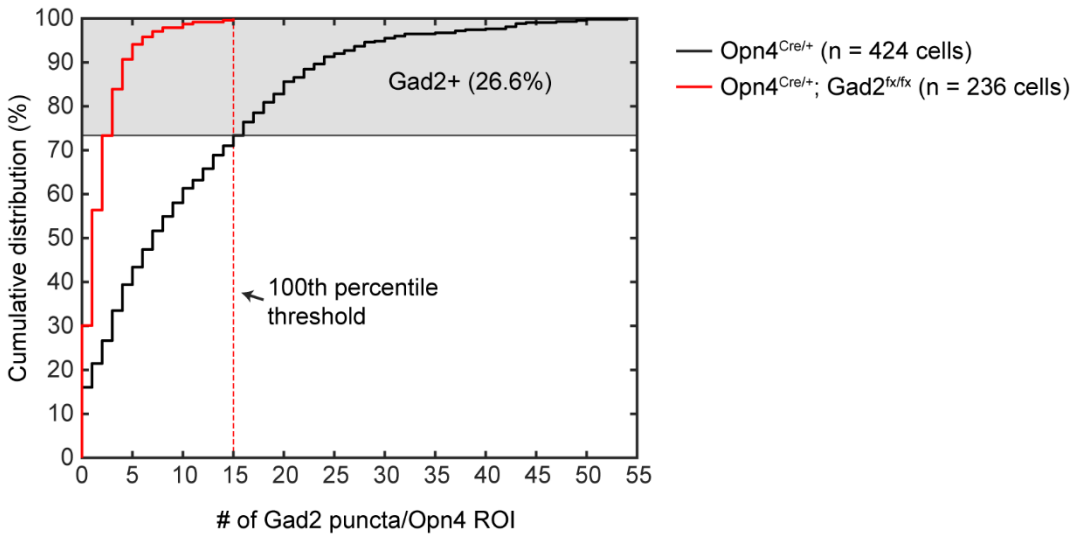

Fig. S7. Quantification of the proportion of Gad2-expressing ipRGCs from RNA fluorescence *in situ* hybridization experiments.

Cumulative distribution plots of the number of Gad2 puncta per Opn4 ROI. Analyses were first performed in Gad2 cKO retinas (*Opn4*$^{Cre/+}$; *Gad2*$^{fx/fx}$, red solid line) to establish a threshold for what can be considered a true Gad2+ ipRGC. The threshold was set at a value which did not include any ipRGCs in Gad2 cKO retinas i.e. the 100th percentile value (red dotted line). The black line represents the cumulative distribution of ipRGCs in *Opn4*$^{Cre/+}$ retinas. 26.6% of ipRGCs contained more Gad2 puncta than the threshold established in Gad2 cKO retinas.

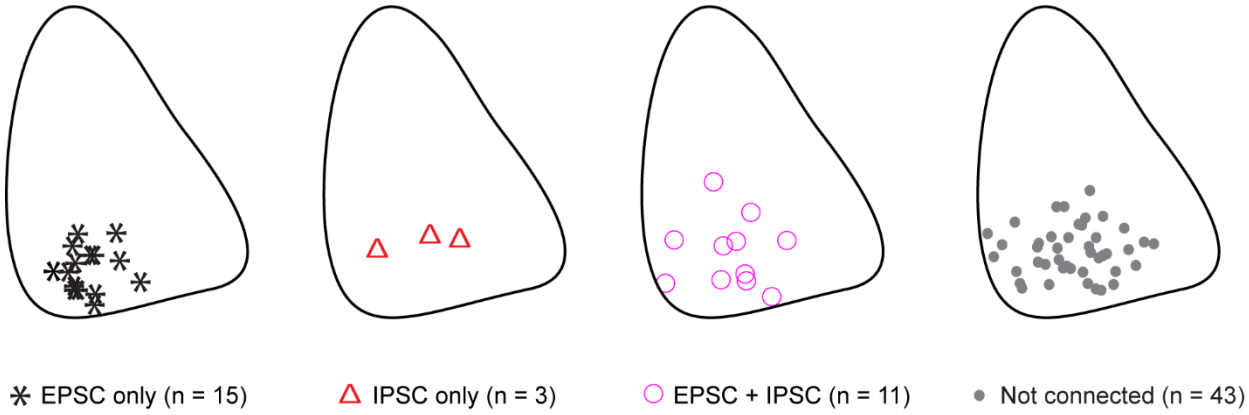

Fig. S8. Location of recorded SCN neurons.

Location of neurons recorded from Ai32 mice eye injected with AAV2/pgk-Cre virus (Fig. 3).

Location was documented in 72/79 recorded neurons.

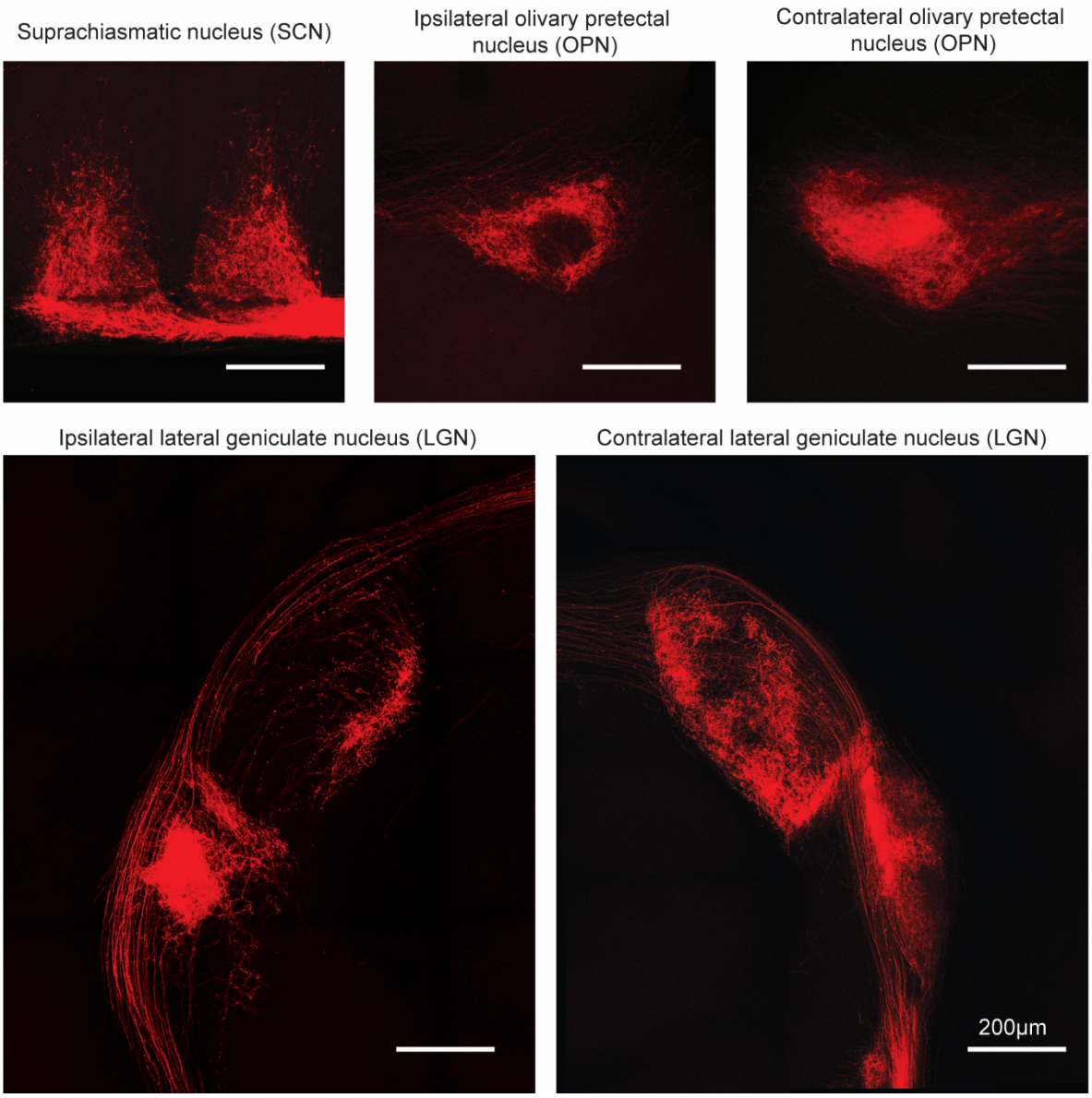

Fig. S9. Central projections of ipRGCs are normal in Gad2 cKO mice.

Example images of ipRGC brain projections in Gad2 cKO (*Opn4*$^{Cre/+}$*; Gad2*$^{fx/fx}$) mice. Unilateral injections of AAV2/hSyn-FLEX-Chrimson-tdTomato were made in *Opn4*$^{Cre/+}$*; Gad2*$^{fx/fx}$ mice (n = 3).

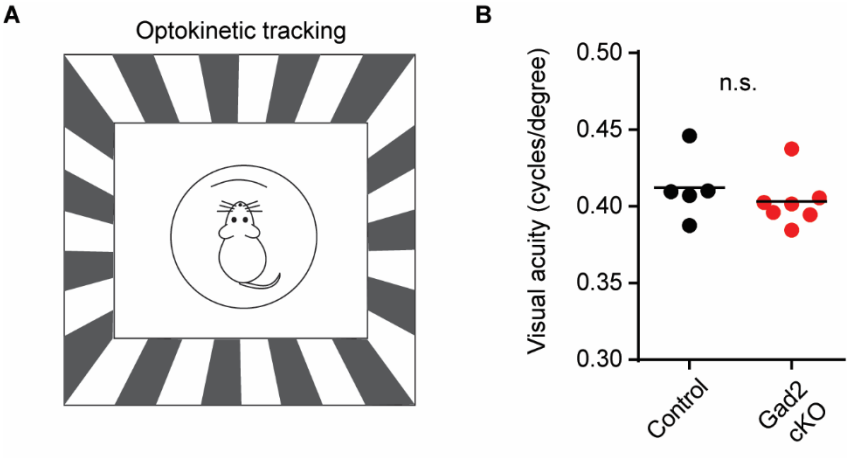

Fig. S10. Gad2 cKO mice have normal visual acuity.

(**A**) Schematic showing the optokinetic tracking (OKT) behavioral assay. Mice were placed on a platform in a chamber surrounded by 4 LCD screens displaying drifting gratings of varying spatial frequency. (**B**) Visual acuity measured by OKT in control (n = 5) and Gad2 cKO (n = 7) mice. n.s. (not significant, Mann-Whitney U test).

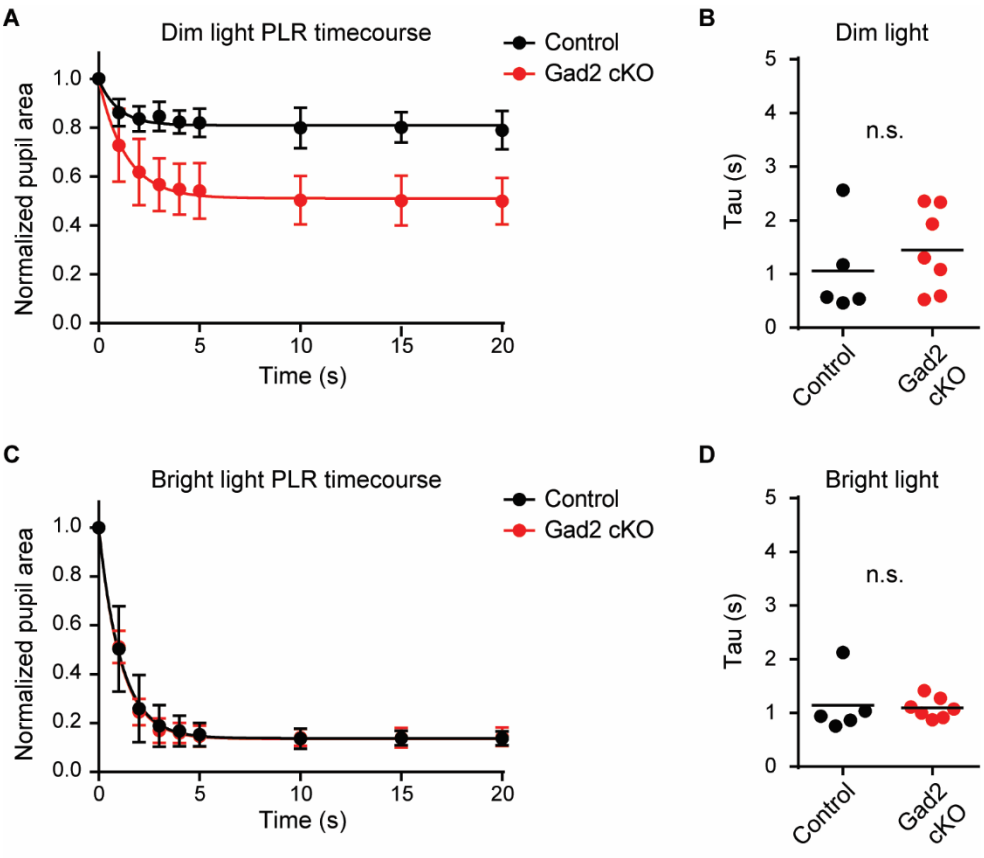

Fig. S11. Time course of PLR in control and Gad2 cKO mice.

(**A and C**) Pupil constriction plotted as a function of time in control (black) and Gad2 cKO (red) mice in response to 20 second dim (10.9 log quanta/cm^2/s, **A**) and bright (13.9 log quanta/cm^2/s, **C**) light stimuli. (**B and D**) Grouped data of the time constant Tau measured by fitting individual PLR data using a single-exponential decay function. There were no significant differences in Tau between control and Gad2 cKO animals in response to dim (**B**) and bright (**D**) light stimuli. n.s. (not significant, Mann-Whitney U test).

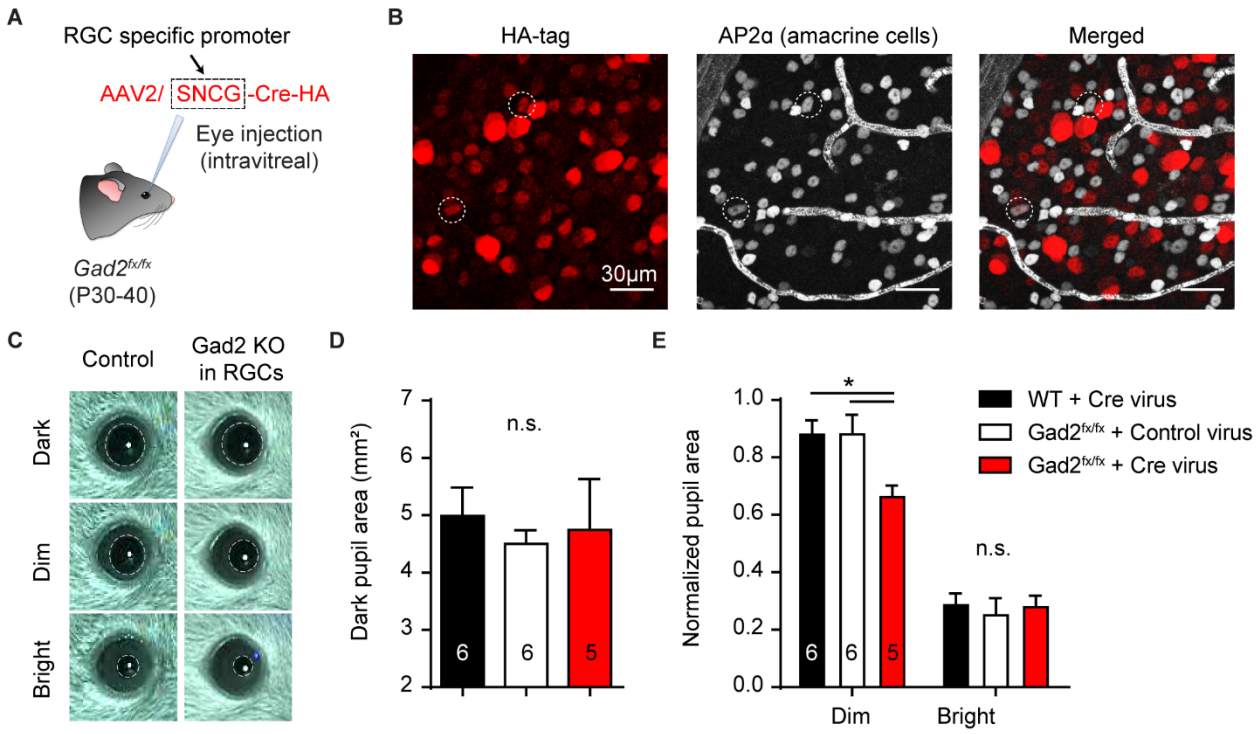

Fig. S12. RGC specific knockout of Gad2 in adult mice results in more sensitive dim light PLR.

(**A**) Schematic showing the experimental approach used to knock out Gad2 specifically in RGCs of adult mice. Adult *Gad2*$^{fx/fx}$ mice were eye injected with a virus that drives Cre expression under an RGC specific promoter (SNCG).

(**B**) Example field of view of retinas immunolabeled for HA-tag (which tags Cre, red) and AP2α (which labels amacrine cells, white). Dotted white circles represent amacrine cells that were positive for HA-tag. 4.59 ± 2.33% of amacrine cells were HA-tag positive (n = 4 retinas, 6554 cells counted total).

(**C**) Representative PLR images from control (left) and experimental mice in which Gad2 was knocked out specifically in RGCs (right).

(**D**) Dark pupil area of control (black and white) and experimental (red) mice. Control groups consisted of WT mice eye injected with SNCG-Cre-HA virus (black) and *Gad2*$^{fx/fx}$ mice eye injected with control virus (SNCG-hPLAP, white). n.s. (not significant, Kruskal-Wallis test). (**E**) Normalized, steady-state constriction of control and experimental mice in response to dim (10.4 log photons/cm^2/s, left) and bright (13.4 log photons/cm^2/s, right) light stimuli. Experimental mice (red) have significantly more constricted pupils in response to dim light, but not bright light. * P< 0.05. n.s. not significant. Kruskal-Wallis test followed by Dunn's multiple comparisons test. Data are mean ± SD.

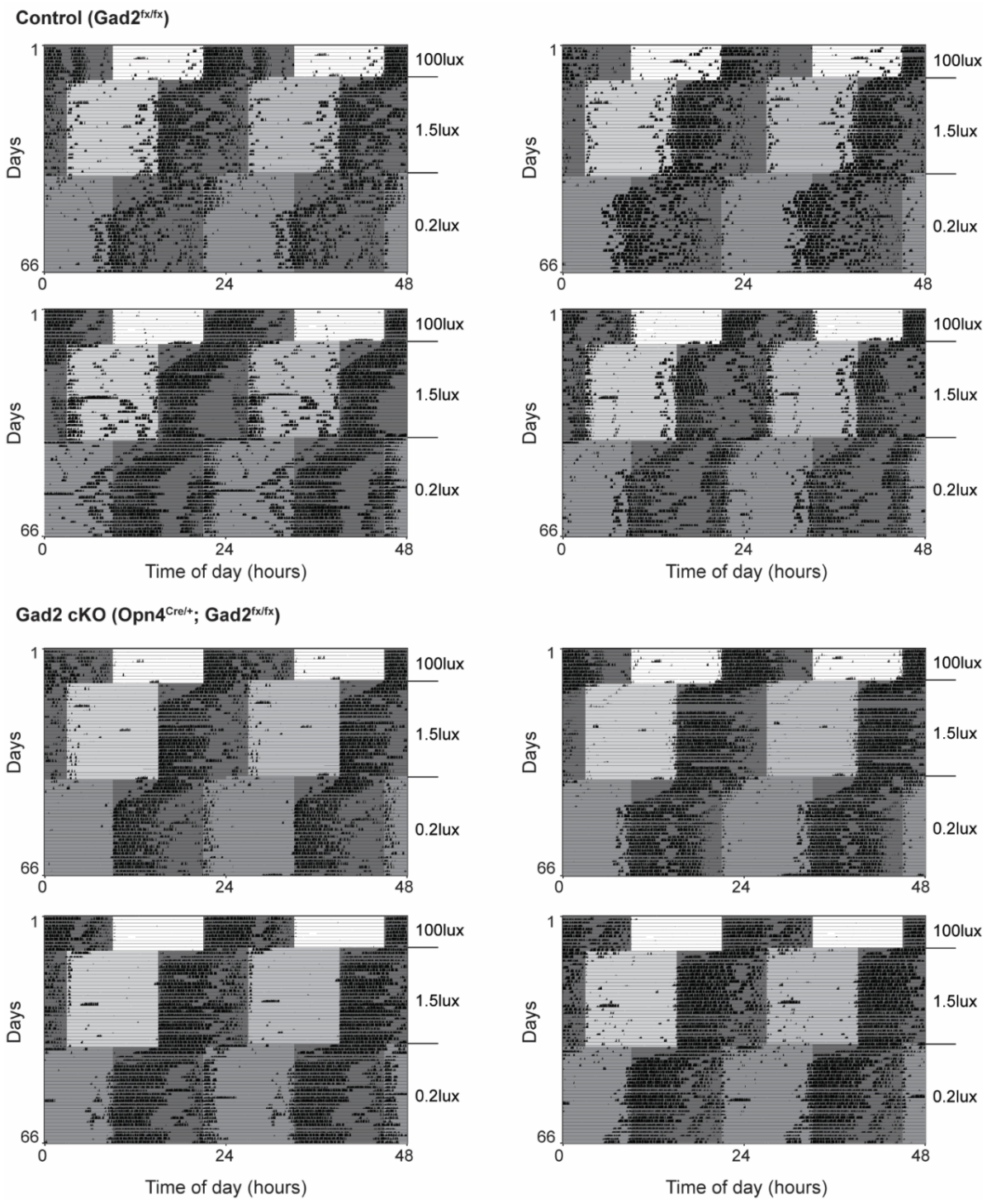

Fig. S13. Representative actograms from control and Gad2 cKO mice.

Representative wheel running activity profiles from control (top) and Gad2 cKO (bottom) mice. The first actogram in each group is the same as actograms shown in Fig. 4.

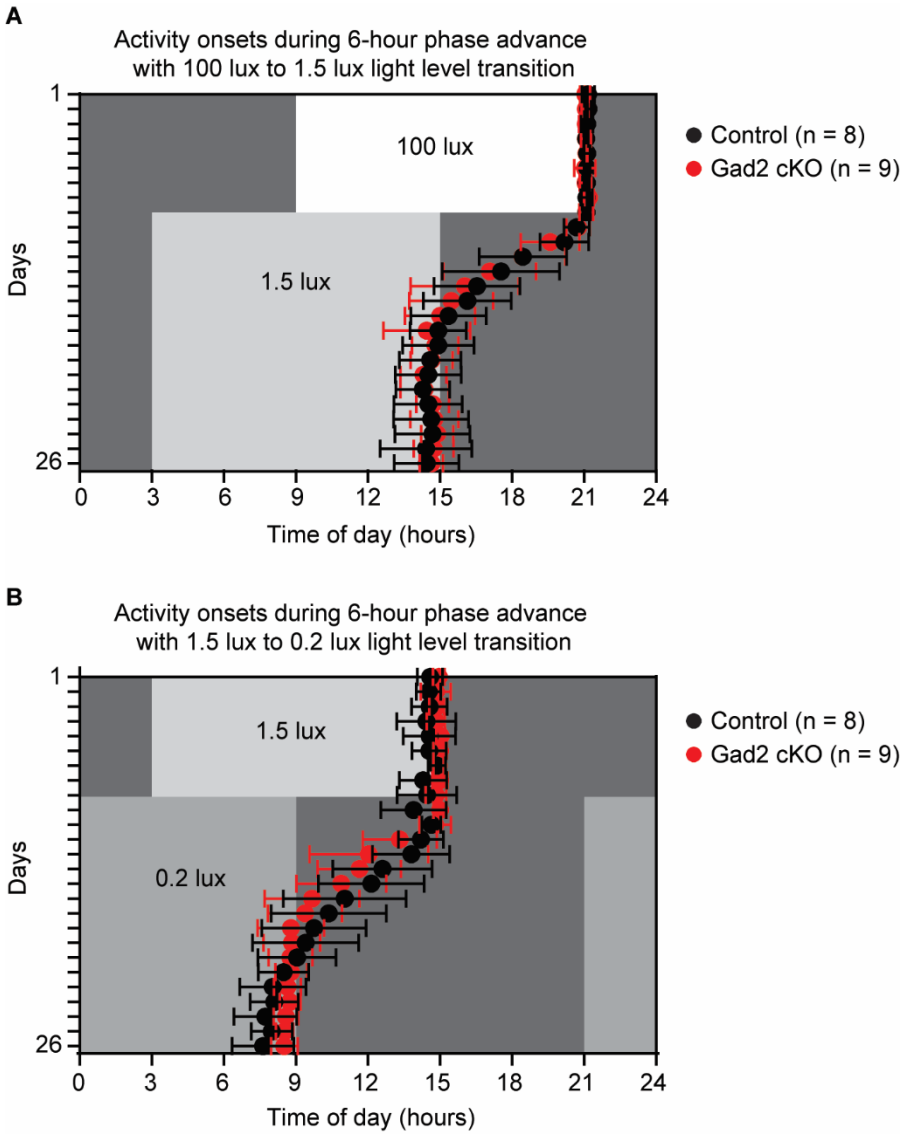

Fig. S14. The rate of re-entrainment to a 6-hour phase advance is normal in Gad2 cKO mice.

(**A-B**) Wheel running activity onsets plotted as a function of days in control (black) and Gad2 cKO (red) mice. Data show onsets 10 days before and 15 days after each 6-hour phase advance. Light levels were decreased from 100lux to 1.5 lux (**A**) and from 1.5 lux to 0.2 lux (**B**) concurrently with each phase advance. Data represent mean ± SD.

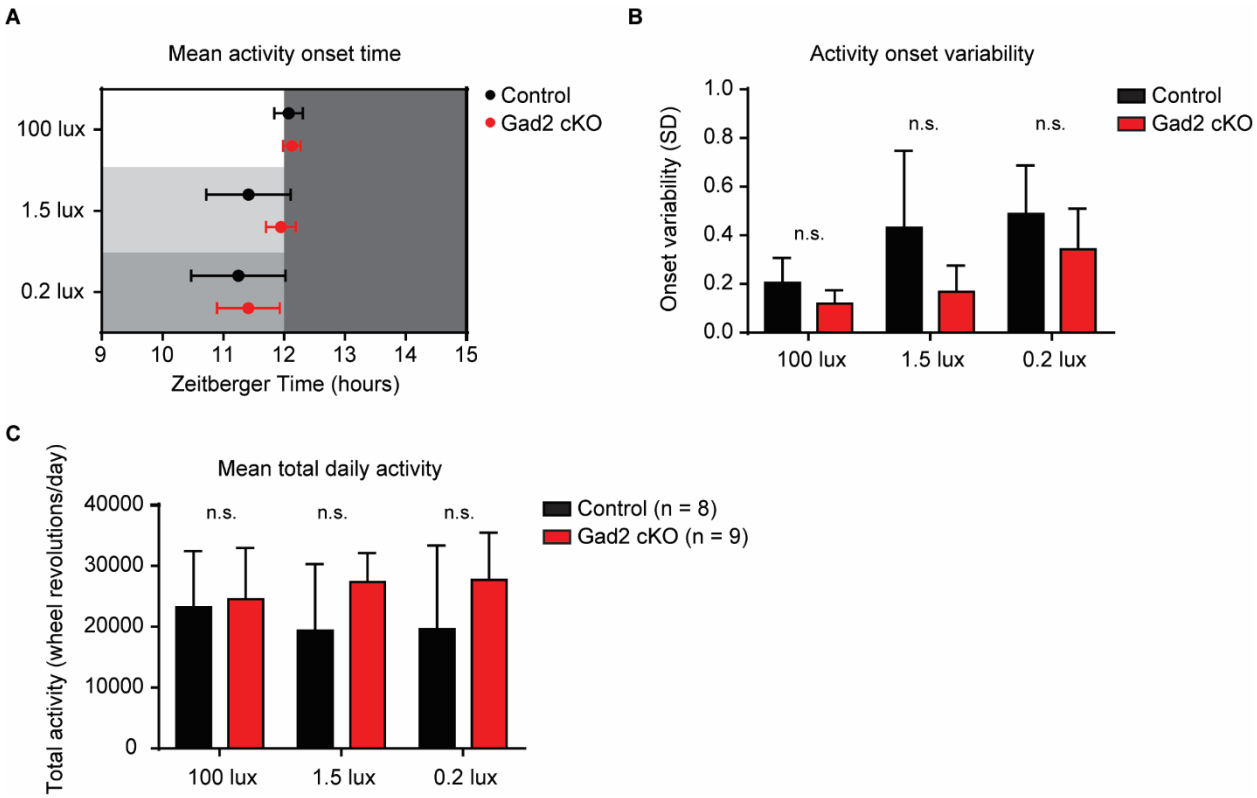

Fig. S15. There are no significant differences in activity onset time, activity onset variability, and total activity between control and Gad2 cKO mice.

(**A**) Wheel running activity onset times in control (black) and Gad2 cKO (red) animals. Lights turn off at 12 hours Zeitgeber time. Onset times were measured by averaging the activity onset times over the 10-day period preceding each 6-hour phase advance. (**B**) Activity onset variability in control and Gad2 cKO mice. Variability was measured by taking the standard deviation (SD) of activity onset times during the 10-day period preceding each 6-hour phase advance. (**C**) Total daily activity in control and Gad2 cKO mice. Total activity was measured by averaging the total wheel revolutions per day over the 10-day period preceding each 6-hour phase advance. n.s. (not significant, Mann-Whitney U test).

References

29. J. T. Ting, T. L. Daigle, Q. Chen, G. Feng, in *Patch-Clamp Methods and Protocols,* M. Martina, S. Taverna, Eds. (Springer New York, New York, NY, 2014), pp. 221-242.

30. R. M. Douglas *et al.*, Independent visual threshold measurements in the two eyes of freely moving rats and mice using a virtual-reality optokinetic system. *Vis Neurosci* **22**, 677-684 (2005).

31. T. M. Schmidt *et al.*, A role for melanopsin in alpha retinal ganglion cells and contrast detection. *Neuron* **82**, 781-788 (2014).